16
Dispersion Interaction and Chemical Bonding

Stefan Grimme

16.1
Introduction

From the various types of chemical bonding discussed in this book, the dispersion bonds are usually considered as being the weakest and therefore the least important for chemistry. This clearly holds true for the strength of a typical atom-pair-wise interaction, which is on the order of 0.5 kcal mol^{-1} or less for molecules composed of light elements ($Z < 40$). The closed-shell rare gas dimers with dissociation energies (D_e) of 0.08, 0.28, and 0.40 kcal mol^{-1} for Ne_2, Ar_2, and Kr_2, respectively, are classical examples. Dispersion interactions can be heuristically defined as the long-range attractive part of the van der Waals (vdW)-type interaction potential between nonpolar atoms and molecules that are not covalently bonded to each other, although the terms ''dispersion'' and ''vdW'' are often used synonymously [1]. Because the term ''dispersion'' has a wide variety of meanings in natural sciences, it is recommended to clearly distinguish it from other, partly related phenomena by using ''London dispersion'' in honor of F. London, who provided the first theory for this interaction [2]. For a detailed discussion of London dispersion (we use from now on the short form) and its relation to noncovalent interactions (NCIs) excellent monographs and review papers are available, for example, Refs. [3–5].

Despite its weakness, the dispersion interaction is extremely important for the formation and structure of many types of condensed matter and the special properties and function of biochemical systems [6–9]. The main reason for this fact is that the dispersion is ubiquitous, always attractive (bonding) and that the interactions are to a good approximation (errors <5–10%) additive. Hence, they add up already in medium-sized molecular systems to values that approach and easily surpass typical covalent and ionic interactions (which are on the order of 100 kcal mol^{-1} per pair interaction). The view that not only rare gas aggregates, liquids or molecular crystals are strongly influenced by dispersion but also chemical bonding and the thermochemistry of common reactions is just emerging [10] (although this idea scatteredly has been proposed much earlier; see, e.g., Ref. [11]; for a related review about closed-shell interactions see Ref. [12]).

The Chemical Bond: Chemical Bonding Across the Periodic Table, First Edition.
Edited by Gernot Frenking, Sason Shaik.

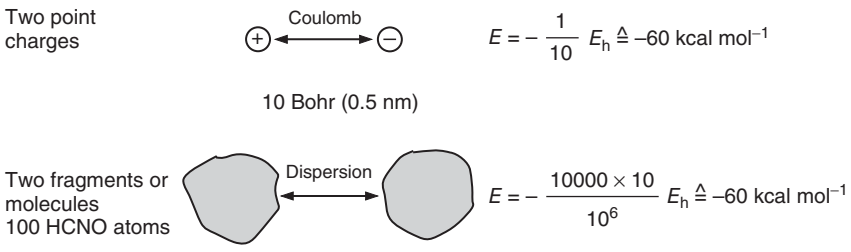

Figure 16.1 Comparison of the magnitude of Coulomb and dispersion interactions. For details, see text.

That dispersion effects are not weak at all can be shown by a simple paper and pencil treatment of model systems (see Figure 16.1) and is later discussed for the bonding in hexaphenylethanes [13] and cation–cation attraction [14] in transition metal complexes.

We take two interacting point charges at a typical distance of 10 Bohr (about 5 Å) as a reference system because its classical electrostatic interaction energy of about 60 kcal mol^{-1} is well conceived by most chemists. This is compared to a medium-sized molecule or aggregate composed of about 200 atoms, which is dissociated into two fragments with 100 atoms each. The number of (dispersion)interacting atom pairs is $100^2 = 10^4$. Taking an average C_6 dipole–dipole dispersion coefficient typical for light (organic) elements (about 10 E_h Bohr^6) and assuming the same (as for the point charges) average interatomic distance between the particles of 10 Bohr, a dispersion interaction energy E_{disp} of about −60 kcal mol^{-1} is obtained, which is close to the corresponding interaction in the electrostatic case. We have made use here of the very fundamental and rather accurate (semiclassical) approximation that the dispersion energy between nonoverlapping fragments consisting of atoms A and B is given by

$$E_{disp} = -\sum_{AB}^{atom\ pairs} \frac{C_6^{AB}}{R_{AB}^6} \tag{16.1}$$

where R_{AB} are interatomic distances and C_6 denotes the pair-specific dipole–dipole dispersion coefficient that determines the interaction strength (and is further discussed later). According to this example, the general consideration of dispersion as being weak is at least misleading when larger molecules interact.

Another aspect of vdW or dispersion bonding is that it generally has the flavor in the literature of being special and totally different from all other types of bonding. While it is certainly true that on an atom-pair-wise basis the interaction is much weaker, the physical mechanisms are not totally different from other more common types of bonding. Phenomenologically, covalent and vdW bonding have more in common than generally thought. This is exemplified by the comparison of the dissociation of the covalent Cl–Cl and dispersive Ar–Ar bond. Corresponding potential energy curves on a reduced energy scale (i.e., scaled to −1 at equilibrium

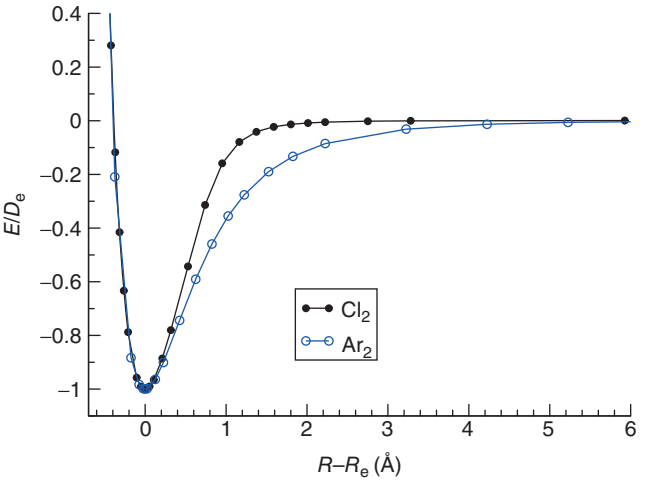

Figure 16.2 Potential energy curves for the dissociation of the covalent bond in Cl_2 (UTPSS-D3/def2-QZVP DFT level of theory) and the van der Waals bond in Ar_2. A reduced interaction energy (i.e., setting the equilibrium value to −1) and shifted distances (setting $R_e = 0$) are given. The absolute D_e values for the two diatomics are 62.2 kcal mol^{-1} (at 2.01 Å) and 0.282 kcal mol^{-1} (at 3.775 Å), respectively, and are in a ratio of a factor of about 210 in favor of the covalent interaction. (Data from [15].)

using E/D_e, where D_e is the equilibrium dissociation energy) and shifted distances with respect to $R_e = 0$ are given in Figure 16.2.

The very similar shape of the two curves, especially in the equilibrium and repulsive regions, is very intriguing. It emphasizes a similar balance of Pauli exchange repulsion (EXR) and attractive interactions, however, at very different distances as the covalent bond is shorter by as much as 1.77 Å. This comparison also clearly shows that the major difference between covalent and dispersion bonding occurs (not unexpectedly) in the asymptotic regime. While the covalent interaction is chemically negligible already at about $R_e + 1.5$ Å (and this holds for many other elements), the dispersion interaction remains significant up to $R_e + 3$ Å.

So, in summary, up to this point the take-home messages are that dispersion interactions are (a) ubiquitous and always attractive, (b) per atom-pair interaction on the order of a factor 100 weaker than covalent ones, (c) more long-ranged (typical distance range of 3-5 Å compared to 1-2 Å for covalent bonds), and (d) additive in character. These properties lead to a wide variety of dispersion bonds and by their admixture to other bonding mechanisms overall to a significant impact in chemistry.

This chapter concentrates on molecular-insulator-type systems that dominate main group inorganic, organic, and biochemistry; and for which dispersion-related phenomena are fairly well understood. For extended metallic systems (but not for many molecular (organo)metallic complexes that are unproblematic) the situation is different, as these have a rather nonlocal (NL) electronic structure and strong

electron correlations appear on all length scales. Special methods and computational tools for dispersion effects with screening for bonding in metals and for molecules on metallic surfaces are just being developed [16–18]. The insulator-type methods as described here will be sufficient for qualitative or semiquantitative purposes also for metals but cannot provide high accuracy (as defined by errors <5–10% for D_e).

After a brief recapitulation of the theory of dispersion interactions in the next section, quantum chemical methods for their accurate computation are described. Because a huge number of different computational schemes have been developed over the years, this chapter cannot be extensive regarding details of the methodology but concentrates on efficient methods for large systems. The last section contains chemical examples that exemplify the sometimes decisive role of the dispersion energy for large chemical complexes.

16.2
A Short Survey of the Theory of the London Dispersion Energy

The dispersion energy is a many-body electron correlation effect and hence appears already for two-electron systems. There is no clear distinction between dispersion and the more conventional electron correlation except that they operate on different interelectronic distance scales (long- and short-ranged, respectively).

In an orbital picture, a single electron occupies some ground-state level. Virtual (unused) orbitals represent excited states (and can be used to construct excited state WF in many-electron cases). Single excitations of the electron to these states change the electronic distribution and when coupled to a corresponding deexcitation, one can think of this process as ''charge fluctuation.'' In a stationary state (time-independent) picture, which is sufficient to understand all dispersion phenomena, these fluctuations actually do not take place but merely represent possibilities. They are realized (as part of the wave function) if a second electron comes into play and then represent electronic correlations, that is, the virtual states (more precisely the corresponding transition densities) interact electrostatically (with exchange-type modifications at smaller distances). The amplitudes of the resulting double-excitations (i.e., coupled single excitations) represent the basic quantity in all wave function theories to compute the dispersion energy. Dispersion is ''transmitted'' by electromagnetic radiation (photon exchange) and not by electron exchange as in covalent bonding such that screening effects in very dense materials (as described by an effective dielectric constant) might appear. Because electronic transition densities (and not charge densities) are the basic quantity for the dispersion bonding mechanism, conventional (charge-density-based) methods of Kohn–Sham density functional theory (DFT) [19–22] have fundamental problems in its description. The characteristic length scale for dispersion interactions can be estimated from the fact that the lowest electric moment of a transition density is of dipole type. The two coupled (induced) dipole moments interact electrostatically via the well-known $1/R^3$ (R being the center-of-charge distance) formula. Because of their mutual (conditional) influence, the corresponding interaction must be

squared in the framework of perturbation theory, leading to the famous $1/R^6$ decay law for the asymptotic part of the London dispersion energy [3]. The interaction between systems in electronically excited states has a dispersion component as well but with different R-dependence and depending on the nature of the state of atoms [23, 24].

Dispersion is omnipresent in electronic systems (such as gravitation in systems with mass) and always attractive (energy lowering). Its natural, also omnipresent, antagonist is the EXR due to the Pauli exclusion principle. It is nowadays clear that any reasonable attempt to quantitatively describe chemical bonding must include these terms together with electrostatic and covalent parts, which, however, still dominate chemical thinking.

The simplest conceivable vdW bond is not represented by the helium dimer (with four electrons) as frequently stated but for triplet dihydrogen (see Figure 16.3). When the Coulomb correlation energy is neglected as in the Hartree–Fock (HF) method, the $^3H_2$ molecule is completely unbound as one electron occupies the bonding σ orbital, while the other is in the antibonding σ^* orbital and the EXR interaction dominates. When the density-dependent, NL VV10 density functional [25] is used with the HF electron density as input (see Ref. [26] for details) and the resulting dispersion energy is simply added to the HF energy, the black-dotted curve in Figure 16.3 results. Comparison of this potential with that given by the C_6/R^6 law (using the exact dispersion coefficient of $6.5E_h$ Bohr^6 for the free hydrogen atom [23]) shows that the potential is essentially dispersion at long range and EXR (exchange repulsion) below $R_e = 4$ Å. Although the "bond" is extremely weak (calculated $D_e = 0.011$ kcal mol^{-1} compared to 0.022 kcal mol^{-1}

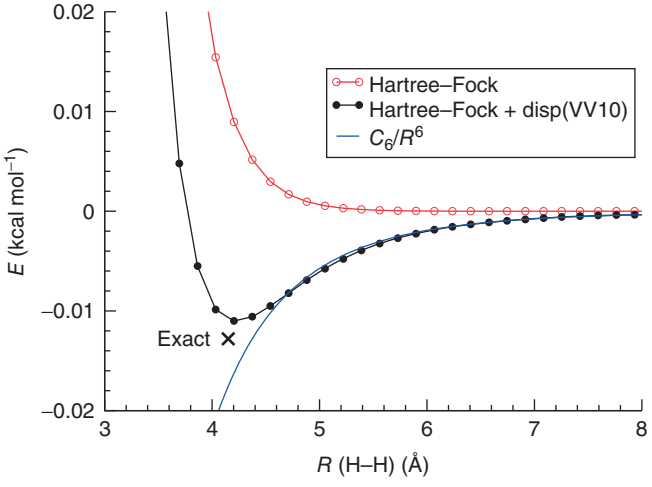

Figure 16.3 Computed potential energy curves for triplet dihydrogen ($^3\Sigma_u$) using the uncontracted aug-cc-pV5Z AO basis. The curve labeled "+disp" is obtained from the Hartree–Fock one by adding the nonlocal correlation energy of the VV10 density functional computed with the SCF density.

for He_2) and very long, this example demonstrates clearly that any two electrons in any state (i.e., with very minor dependence on the electron spin) can exhibit the phenomenon of dispersion binding. The practically exact values [27] for this system are 0.013 kcal mol^{-1} and 4.15 Å for D_e and R_e, respectively, which are in good agreement with the HF-NL data. Note that the $^3\Sigma$ state is an excited one (the ground state cannot be used here because the covalent bond formation would dominate the potential on the energy scale shown) and this example hence indicates that the VV10 functional seems to be applicable for excited states as well (it has so far only been employed for ground states).

The situation in more interesting, larger chemical systems is of course much more complex and a simplified analysis for understanding is appropriate. The energy decomposition analysis (EDA) is a valuable theoretical tool to partition the interaction energy from a supermolecular self-consistent field (SCF)-type computation into physically meaningful components [28]. It goes back to Morokuma [29, 30] and recently has proved to give detailed information about the nature of chemical bonding [31] as well as for the interactions in hydrogen-bonded systems [32], supramolecular structures [33] and vdW complexes [34]. The formation of bonding between two fragments is divided into three physically plausible steps. In the first step, the fragment electronic densities (in the frozen geometry of the supermolecule) are superimposed, which yields the quasi-classical electrostatic interaction energy (ES). Renormalization and orthogonalization of the product of monomer wave functions yields the repulsive energy term EXR. In the final step, the molecular orbitals are allowed to relax to their final form variationally. This yields the (usually stabilizing) induction energy (IND), the orbital interaction (covalent, COV) and charge-transfer terms (CT). The dispersion energy is calculated with the D3 approach (see subsequent text). Here, we do not discuss all these energy components of the partitioned total interaction energy ΔE in detail but concentrate on the three quantities

$$\Delta E = E_{\mathrm{EXR+ES}} + E_{\mathrm{CT+IND+COV}} + E_{\mathrm{disp}} \tag{16.2}$$

which describe (in the above-mentioned order) (a) semiclassical (steric) interaction, (b) ''true'' chemical bonding and (c) dispersion. Their sum differs from the exact interaction only by the energy necessary to bring the optimum monomer geometries into the form they have in the supermolecule. Because we employ frozen monomer geometries, this deformation (also called preparation) energy contribution vanishes. It is generally small (<2–3% of D_e) in noncovalently bound complexes and can be neglected to a good first approximation.

As an example, the results for formation of the donor–acceptor bond in Me_3N-BMe_3 are shown in Figure 16.4. Such bonds (and their strengthening by dispersion and weakening by EXR effects) play an important role in the so-called frustrated Lewis pairs (FLP), which have attracted enormous attention recently because of their ability to activate small molecules such as H_2 [35–37]. Because the bond dissociates heterolytically into closed-shell fragments, static electron correlation effects play no important role and a standard restricted DFT treatment

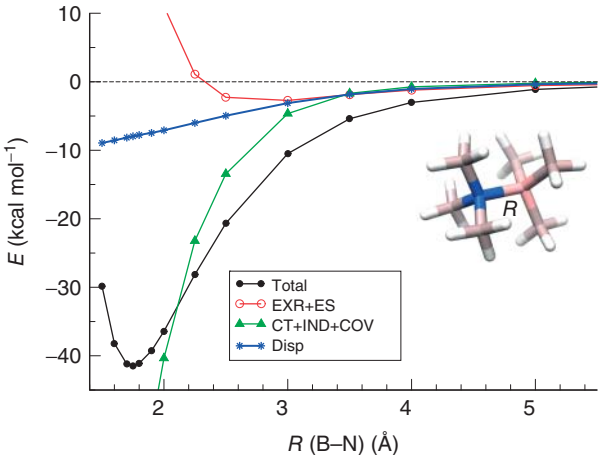

Figure 16.4 Energy decomposition analysis (EDA) at TPSS-D3/def2-TZVP level for donor–acceptor bond formation in Me_3N-BMe_3 (rigid fragment approximation). For a definition and explanation of the energy terms, see text.

is appropriate. In most of the following examples, the TPSS [38] meta-GGA density functional and the Ahlrichs-type def2-TZVP [39, 40] Gaussian atomic orbital (AO) basis is used. This level of theory has proved to be generally robust in hundreds of applications and large-scale benchmarks [41] with a very good performance/computational cost ratio.

As can be seen in the plot, the medium-sized interaction (D_e = 42 kcal mol^{-1}) in the equilibrium region and for slightly larger distances up to 2.5 Å is dominated by chemical bond formation ($E_{COV+IND+CT}$ term). Because the Me_3N and BMe_3 fragments have low polarity and are somewhat bulky (similar to many FLPs), the E_{EXR+ES} term is only weakly bonding and at short distances strongly repulsive (“steric hindrance”). For long bond distances, all three components contribute about equally to binding. Dispersion is rather attractive and adds 5–10 kcal mol^{-1} in the equilibrium region, which is about 10–20% of D_e already for the relatively small methyl substituents considered here. For realistic FLPs where large mesityl and C_6F_5 substituents are present, the corresponding dispersion contributions can reach 30–40 kcal mol^{-1} and more than 100% of D_e [36]. This example shows that already for systems with eight nonhydrogen atoms and for conventional bond formation dispersion effects play a nonnegligible role and must be considered in accurate work.

Many of the more conventional bonding types in chemistry can vary considerably for elements across the periodic table. One of the questions in this context is how far this holds for dispersion binding or the contribution of dispersion to other bonds. As Eq. (16.1) suggests, a good measure for the strength of the dispersion interaction between two atoms AB is their C_6^{AB} coefficient. To a good approximation, it can be taken as the average (arithmetic or geometric) of the values of the corresponding

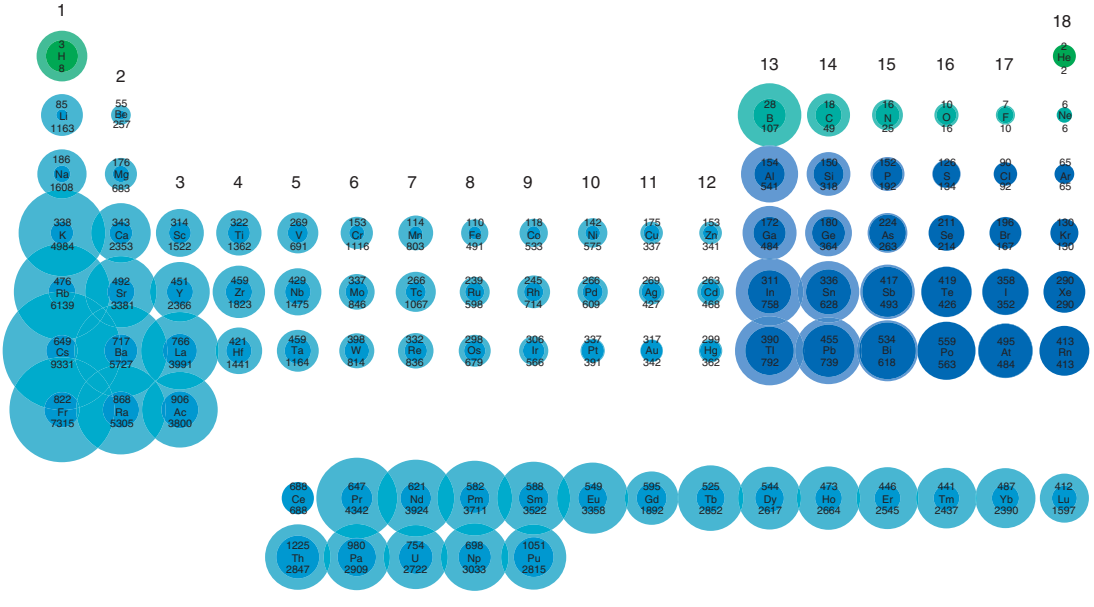

Figure 16.5 Computed (TDDFT/PBE38) C_6 dispersion coefficients (in E_h Bohr^6) for the whole periodic table (up to Pu), which are used in the DFT-D3 method. For each element the free atom value (lower value, light colored circle) and the coefficient (upper value, darker color) for the atom in a saturated chemical environment (with the highest coordination number according to the DFT-D3 scheme, e.g., four for carbon and three for nitrogen) are given. The radius of the circle is proportional to $C_6^{1/3}$. Scale factors for better visibility are 15 (H–He), 5 (B–Ne) and 2 (rest of the III–VIIIa elements).

C_6^{AA} and C_6^{BB} coefficients. As a valuable spin-off product from the development of the D3-method [42], these data were consistently computed for the whole periodic table and part of the results are shown in Figure 16.5. Given are the C_6^{AA} values for the free atoms and for the atom in a chemically saturated environment, that is, when the atom has used all of its ''normal'' valencies (e.g., four and two for carbon and oxygen, respectively) for covalent bonding. These values are based on first-principles time-dependent density functional theory (TDDFT) computations of frequency-dependent polarizabilities, as pioneered by the Baerends group [43, 44]. For other recent studies on the dependence of the C_6^{AB} coefficients on the chemical environment, see Ref. [45]; for a discussion of relativistic effects, see Ref. [46].

As can be clearly seen (by comparison of the size of the circles), the free atom and bonded atom values can differ by large amounts, in particular for the alkaline and earth alkaline metals. Their bonding is associated more or less with oxidation, and the loosely bound valence electron (responsible for the high polarizability of the free atom) is ''lost'' for dispersive bonding. This quenching of the free atom dispersion in molecules is less pronounced for nonmetals and weakens to the right in the periodic system of elements (PSE). Physically it is related to the increase in electronic excitation energies by covalent bond formation (widening of HOMO–LUMO gap). Very significant changes are still observed for carbon, for which the values decrease from 49 to about 18 (all values in atomic units in the following) in the typical sp^3 molecular valence state. This property is very important for the subtleties in dispersion binding of carbon-rich materials of saturated and unsaturated character [47]. In the D3 method (see subsequent text), the dispersion quenching with the increasing number of bonds formed is accounted for by a geometrically computed, continuous and fractional coordination number. Within one group of elements the relative difference between maximum and minimum atomic C_6 values typically decreases, for example, from 25 to 16 for N, from 192 to 152 for P, and from 263 to 224 for As. For the heavier halogens, maximum and minimum values are essentially the same, which is consistent with the view that the quenching effect of the single unpaired electron and the increase in the C_6 value by electron acceptance in a single (mostly ionic) bonding almost cancel.

The about 33 000 C_6^{AB} coefficients that were computed for the D3-method [42] as supporting points for interpolation of C_6 values in molecules enable us not only to accurately compute the dispersion energy for atoms in different molecular environments but also lead to a detailed understanding of dispersion bonds.

16.3 Theoretical Methods to Compute the Dispersion Energy

Because the dispersion energy is an essential part of NCIs and this topic is nowadays in the focus in various areas of chemistry and physics, excellent reviews already exist [48] and only a brief summary and recapitulation is given here.

16.3.1 General

Currently there are only three basically different *ab initio*-type methods in use (the vast amount of empirical potentials is not considered here). These are

1) Supermolecular by wave function theory (WFT);
2) Supermolecular by DFT with dispersion corrections;
3) Symmetry-adapted perturbation theory (SAPT) based on fragments.

Supermolecular methods compute the interaction ΔE (and their parts, e.g., dispersion) as a difference of total energies E_{tot} for the aggregate (complex AB) and the fragments (A and B) as

$$\Delta E = E_{tot}(AB) - E_{tot}(A) - E_{tot}(B) \tag{16.3}$$

The approach has the advantage that any approximate electronic structure method from WFT or DFT can be used in Eq. (16.3). The dispersion energy can be treated separately as, for example, in dispersion-corrected DFT (or HF)

$$E_{tot} = E_{SCF} + E_{disp} \tag{16.4}$$

where E_{SCF} is the conventional Kohn–Sham (or HF) SCF electronic energy and E_{disp} is the dispersion correction. Note that we use here the terms interaction energy (ΔE) and dissociation energy (D_e) synonymously, although they have different signs and more precisely differ by the fragment relaxation energy (included in D_e, i.e., it is observable when zero-point vibrational energies are added, while relaxation is neglected for ΔE; for diatomics $\Delta E = -D_e$ holds). This allows a convenient computation of the dispersion contribution to binding, that is, ΔE_{disp} according to Eq. (16.3). Because $E_{tot}(AB)$ is explicitly computed, intramolecular NCI and dispersion effects can be obtained if a proper reference state (e.g., folded vs unfolded conformation) can be defined. A disadvantage of the supermolecular approach is that it is contaminated with the so-called basis-set superposition error (BSSE), a one-particle basis incompleteness effect, which is severe especially in correlated WFT calculations with small or medium-sized AO basis sets. For DFT or HF calculations with triple-zeta basis sets, it is typically only <5–10% of D_e (<2–3% with quadruple-zeta basis sets) and negligible when compared to other more important sources of error (e.g., the approximate nature of the exchange-correlation functional in DFT) [49]. For a recent in-depth discussion of the BSSE in the framework of DFT, see Ref. [50]

16.3.2 Supermolecular Wave Function Theory (WFT)

Because dispersion is a genuine electron correlation effect, a common approximation in WFT is to compute it as

$$\Delta E_{disp} \approx \Delta E_c = \Delta E_{post\,HF} - \Delta E_{HF} \tag{16.5}$$

where ΔE_{HF} is the HF interaction energy and $\Delta E_{\mathrm{post\,HF}}$ refers to a correlated WFT treatment such as Moeller-Plesset second-order perturbation theory (MP2) or coupled-cluster with single and double excitations (CCSD(T)) with correlation energy E_{c} [51]. This approximation works fairly well for large interfragment distances but is obscured for shorter bonds by exchange and intrafragment correlation effects.

An appealing feature of this partitioning is that the correlation (dispersion) energy computationally can be assigned exactly to contributions from orbital pairs. If localized molecular orbitals (LMOs) are used in the correlation treatment, this allows a local (group- or fragment-wise) description of dispersion effects [52]. The correlation energy (E_{c}) for an HF reference state can be written as a sum over occupied orbital pairs ij

$$E_{\mathrm{c}} = \frac{1}{2}\sum_{ij} e_{ij} \tag{16.6}$$

In the simplest correlated WFT, which is second-order Møller–Plesset perturbation theory (MP2) [53, 54], the pair energies e are given by a sum over all virtual orbital pairs ab

$$e_{ij} = -\sum_{ab} \frac{(ia|jb)[(ib|ja) - (ia|jb)]}{\varepsilon_i + \varepsilon_j - \varepsilon_a - \varepsilon_b} \tag{16.7}$$

Here, ε are canonical HF eigenvalues and $(ia|jb)$ are two-electron integrals in charge-cloud notation. For modern, improved versions of MP2, see Ref. [55]. Because E_{c} is invariant under unitary transformations within the occupied and virtual orbital blocks for common approximations (e.g., MP2 or CCSD), identical results compared to the canonical treatment are obtained when the orbitals ij are replaced by LMO. Because LMO are usually strongly localized on atoms or in chemical bonds (mostly to >95% on <2–3 atoms), it is possible to partition the total correlation energy into chemically meaningful inter- and intrafragment contributions according to

$$E_{\mathrm{c}}(\mathrm{inter}) = \sum_{i\subset F_1}\sum_{j\subset F_2} e_{ij} \tag{16.8}$$

$$E_{\mathrm{c}}(\mathrm{intra}) = \frac{1}{2}\sum_{ij\subset F_1} e_{ij} \tag{16.9}$$

Here, F_1 and F_2 denote sets of orbitals that define molecular fragments or orbital spaces (i.e., core, σ, π, lone-pair). The decision on the type of orbital and the atom to which it belongs can (automatically) be made on the basis of a Mulliken population analysis [56] of the LMO in question. Asymptotically, when fragments F_1 and F_2 are spatially well separated, the interfragment correlation energy is equal to the interaction energy, which can be further interpreted as their dispersion interaction

$$E_{\mathrm{c}}(\mathrm{inter}) \approx E_{\mathrm{disp}} = -\frac{C_{\infty}^{F_1F_2}}{R^n} \tag{16.10}$$

Here, $C_{\infty}^{F_1F_2}$ denotes an effective dispersion coefficient for the fragments, R is their (center-of-charge) distance and n is an effective exponent typically close to six.

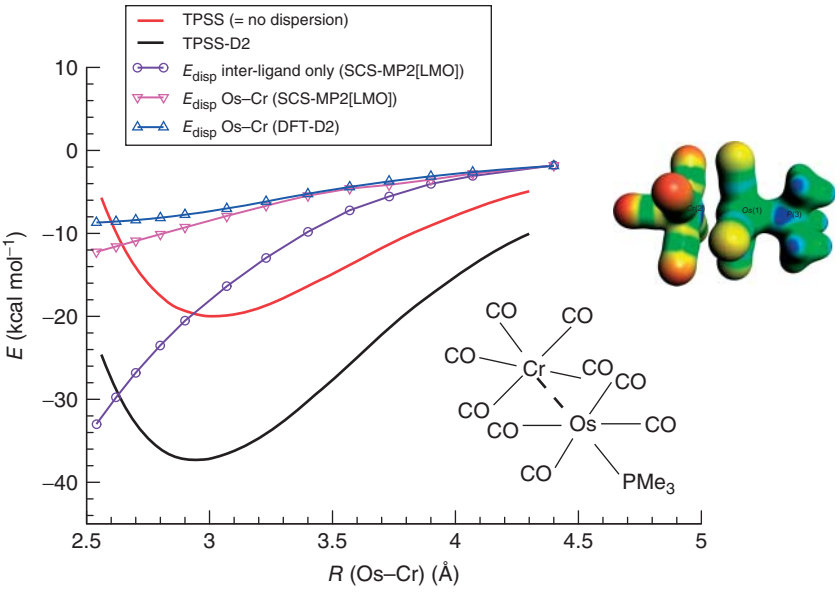

Figure 16.6 Computed• potential energy curves for the Os–Cr interaction in $(OC)_5Cr\text{-}Os(CO)_4PMe_3$ from Ref. [57]. The graph shows a comparison of TPSS and TPSS-D2 curves corresponding to a large dispersion contribution to binding and two contributions to the interfragment dispersion energies at the partitioned spin-component-scaled (SCS)-MP2(LMO) level. Note the relatively small dispersion interaction (triangles) between the metal atoms (and the good agreement of SCS-MP2(LMO) and DFT results for this) and the dominant ligand–ligand (i.e., CO and PMe_3) contribution (circles). The inset shows a color-coded map of the molecular electrostatic potential on an iso-charge-density surface, indicating no significant electrostatic interaction (small polarity) as well as almost no overlap-based bonding interaction between the Os and Cr atoms. The Os–Cr bond is considered as being mainly dispersion driven with some short-range correlation effects that are captured by the density functional.

Note that the effective dispersion coefficient also contains higher order moments than the usual induced dipole–dipole term because the full electric moments of the LMOs are considered by the integrals in Eq. (16.7).

A recent example for this type of analysis in a donor-acceptor-type transition metal complex [57] is given in Figure 16.6; for other applications in the field of biochemical model systems, see Refs. [52, 58].

16.3.3
Supermolecular Density Functional Theory (DFT)

Dispersion corrections to DFT and HF (including semiempirical methods) have recently been reviewed [59, 60] and hence only a brief description is given. Asymptotically correct approaches are either atom-pair-based (e.g., DFT-D3 [42], XDM [61], or Tkatchenko-Scheffler (TS)-vdW [62]) or compute the dispersion energy from the electron density (called vdW-DF [25, 63]). For recent work on the

combination of dispersion and long-range exchange corrections, see Ref. [64]. A new idea for a NL dispersion correction was proposed recently by Hesselmann [65].

In the general vdW-DF framework, such an NL correlation (dispersion) energy takes the form of a double-space integral

$$E_{\text{disp}}^{\text{NL}} = \frac{1}{2}\iint \rho(r)\phi(r,r')\rho(r')\text{d}r\text{d}r' \tag{16.11}$$

where ρ is the charge density and r and r' denote electron coordinates. The different variants of vdW-DF that are currently on the market only differ in the choice of the NL correlation kernel $\phi(r,r')$. These kernels are physically based on local approximations to the (averaged) dipole polarizability at frequency ω (i.e., $\alpha(r,\omega)$). Knowing ω at all (imaginary) frequencies leads automatically, via the famous Casimir–Polder relationship [66] given in Eq. (16.12), to the long-range part of the dispersion energy. This clarifies the deep relation to atom-pair-wise methods that employ these coefficients as basic quantities and replace the charge density by atom-centered delta functions and the double-integral by a double sum. The C_6 dispersion coefficient for induced dipole–dipole dispersion interacting fragments A and B is given by

$$C_6^{\text{AB}} = \frac{3}{\pi}\int_0^\infty \alpha(i\omega)^A\alpha(i\omega)^B d\omega \tag{16.12}$$

Higher order dipole–quadrupole, quadrupole–quadrupole, … coefficients (i.e., C_8, C_{10}, …) can also be computed by similar formulas [3]. Odd-order terms vanish for spherical systems (free atoms) but occur for nonspherical ''atoms'' as found in molecular environments. It is currently not clear how large the effect of including, for example, C_7 really is [67], but so far very good results have been obtained by including even-order terms only.

The C_6 coefficients (and derived C_8) in the D3 method have been computed using a modified form of this relation, where the $\alpha(i\omega)$ are computed nonempirically by TDDFT and A and B are reference molecules from which atomic values are derived [42]. Because the reference system can also be a molecular cluster modeling a solid environment, special coefficients for atoms in the bulk can be derived [68]. The final form for the DFT-D3 two-body part of the dispersion energy employs the so-called Becke–Johnson (BJ) damping [61, 69] and truncates the expansion at C_8

$$E_{\text{disp}}^{\text{D3(BJ)}} = -\frac{1}{2}\sum_{\text{A}\neq\text{B}}\frac{C_6^{\text{AB}}}{R_{\text{AB}}^6 + f(R_{\text{AB}}^0)^6} + s_8\frac{C_8^{\text{AB}}}{R_{\text{AB}}^8 + f(R_{\text{AB}}^0)^8} \tag{16.13}$$

where $f(R_{\text{AB}}^0) = a_1 R_{\text{AB}}^0 + a_2$ and a_1, a_2, and s_8 are empirical parameters that have been determined by a fit to CCSD(T) interaction energies for typical NCI (i.e., the S66 set [70]). The vdW-DF method in the VV10 flavor also contains two empirical parameters (adjusting the long- and short-range behavior) of which only the latter is fitted for each density functional [26].

This form of the damping function ensures that for small interatomic distances the right constant limit for the energy correction is obtained [71]

$$E_{\text{disp}} = -k_1 + k_2 R_{\text{AB}}^2 \ (R_{\text{AB}} \to 0) \tag{16.14}$$

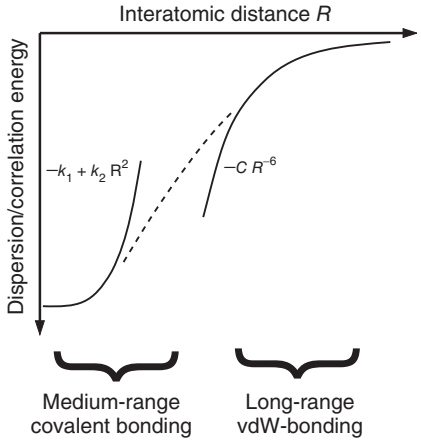

Figure 16.7 Schematic description of the long- and medium- or short-range behavior of the dispersion/correlation energy.

where k_1 and k_2 are atomic constants. This behavior (which is also fulfilled by the vdW-DF method using the VV10 kernel [25]) is the reason why dispersion in a broader sense of definition can influence ''normal'' bonding (thermochemistry). When atoms come close together, the electrons can be still far apart (i.e., showing long-range dispersion-type correlations) and hence dispersion becomes part of the ''normal'' correlation energy. This is illustrated in Figure 16.7. The D3- and NL corrections have been carefully benchmarked on a very large variety of NCI [26, 42, 72, 73] and, in general, high-accuracy (errors <10% of D_e) and only small variations between the different methods have been observed. This is documented here on a very recent, more difficult example of interacting metal atoms. The dimer of the so-called oxaliplatin complex (a potent anticancer drug [74]) is investigated along a rigid dimerization coordinate (for the structure, see inset in Figure 16.8). Although the complex is considered as being strongly hydrogen bonded, by comparison of the uncorrected TPSS and TPSS-D3/NL curves the strong effect of dispersion (about 20 kcal mol^{-1} binding, see Figure 16.8) becomes apparent. As mentioned, the agreement between D3 and NL results is excellent.

16.3.4
Symmetry-Adapted Perturbation Theory (SAPT)

The methods based on SAPT are conceptually different from the supermolecular approaches because they require the definition of fragments and do not compute the total energy, but distinct interaction energy components including dispersion. For an excellent review about the theory, the various versions of SAPT and also for technical aspects, see Ref. [75]. The word symmetry here refers to the Fermionic-antisymmetry of the WF, meaning that the Pauli principle is included, which is not straightforward when the starting points of the description are separate molecular or atomic fragments. The partitioning of the system is mapped to a partitioning of

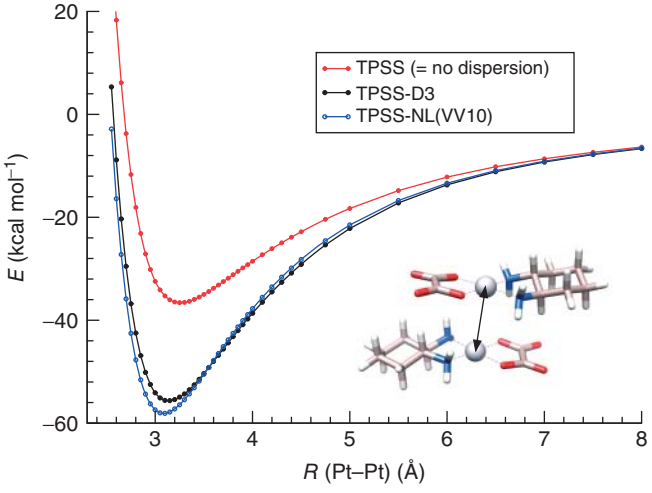

Figure 16.8 Computed potential energy curves for the oxaliplatin complex (TPSS density functional, def2-TZVP AO basis, large core (Cologne–Stuttgart) ECP for Pt.

the Hamiltonian into fragment (index A or B) and interaction operators

$$\hat{H} = \hat{H}(\mathrm{A}) + \hat{H}(\mathrm{B}) + \hat{V}(\mathrm{AB}) \tag{16.15}$$

where $\hat{V}(\mathrm{AB})$ contains all intermolecular Coulomb interactions. SAPT requires the choice of a quantum chemical method for the monomers, that is, HF, DFT, or CC methods. Applying perturbation theory leads to energy contributions in different orders, which add to the total interaction energy $\Delta E_{\mathrm{int,\,AB}}$ according to

$$\Delta E_{\mathrm{int,\,AB}} = E_{\mathrm{ES}}^{(1)} + E_{\mathrm{EXR}}^{(1)} + \underbrace{E_{\mathrm{IND}}^{(2)} + E_{\mathrm{EXR-IND}}^{(2)}}_{E_{\mathrm{IND}}} + \underbrace{E_{\mathrm{disp}}^{(2)} + E_{\mathrm{EXR-disp}}^{(2)}}_{E_{\mathrm{disp}}} + \ldots \tag{16.16}$$

Usually, the expansion is truncated at second order and the mixed $E^{(2)}$ terms are condensed, yielding a formula which resembles that of the EDA

$$\Delta E_{\mathrm{int,\,AB}} = E_{\mathrm{EXR}} + E_{\mathrm{ES}} + E_{\mathrm{IND}} + E_{\mathrm{disp}} \tag{16.17}$$

SAPT is not applicable to intramolecular interactions, but has the advantage of being free of BSSE. It likely provides the theoretically best-founded definition of the dispersion energy in the overlapping regime. For large distances, its description resembles the Casimir–Polder formula with monomer polarizabilities from the chosen method. On average, the accuracy for NCI is much better than that of MP2 and reaches that of the supermolecular CCSD(T) "gold standard," at least when DFT is used as an inherent method and extended AO basis sets are used [76]. For recent further developments of SAPT for large systems, see, for example, Refs. [77, 78].

16.4
Selected Examples

16.4.1
Substituted Ethenes

Steric hindrance is a widely used concept in chemistry. Normally, it is stated that spatially close-lying functional groups (typically alkyl like *t*-butyl) try to avoid each other (because of the EXR + ES term) and prefer large interfragment distances. Note that this is expected to lead to weaker bonds in the core of the corresponding chemical system, that is, a kinetic stabilization but thermodynamic destabilization. That this is only part of the story is exemplified by our first example. The dissociation energy of the central CC bond in tetrasubstituted ethenes (see Figure 16.9) is considered. The common view holds true when the four substituents in ethene are increased in size from methyl to *i*-propyl and 3-pentyl, for which the D_e values decrease monotonously from about 170 to 140 kcal mol^{-1}. However, further increase of "steric hindrance" increases the D_e again! Note that this effect is completely missing when the D3 correction is omitted in the DFT calculations and hence can be clearly attributed to an increasing dispersion attraction by the long alkyl chains. The effect is chemically significant and amounts to about 10 kcal mol^{-1}

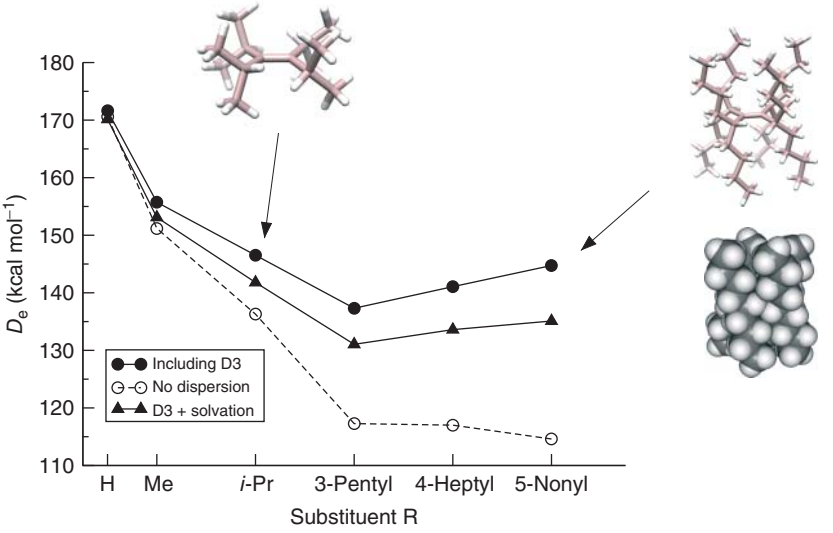

Figure 16.9 Dissociation energy D_e for the central CC bond in tetrasubstituted ethenes $R_2C = CR_2$ at (U)TPSS-D3/def2-TZVP levels. Open circles denote data from single-point calculations without D3 dispersion corrections and illustrate the dramatic effects of the dispersion energy for the larger systems. Results including enthalpic (298 K) corrections for solvation in $CHCl_3$ (gray triangles) are obtained from the conductor-like screening model for realistic solvents (COSMO)-RS [79–81] model (employing DFT input data).

relative stabilization from 3-pentyl to 5-nonyl. It is weakened but persists even when the system is treated in solution by a continuum model (COSMO-RS).

16.4.2
Steric Crowding Can Stabilize a Labile Molecule: Hexamethylethane Derivatives

The stabilization of normal covalent bonds by dispersion in large systems is rather obvious from the last example and those given in Ref. [10]. Very recently, we could furthermore show that there are cases in which the dispersion between seemingly ''innocent'' ligands provides the main driving force for binding, meaning that without these forces the system would spontaneously dissociate. We consider the textbook example of hexaphenylethane (see inset in Figure 16.10 for the structures) and its inability to form a stable CC single bond [13]. A delicate balance of covalent bonding, dispersion attraction, and Pauli repulsion forces between the phenyl rings and attached substitents can be expected when the central CC bond is broken.

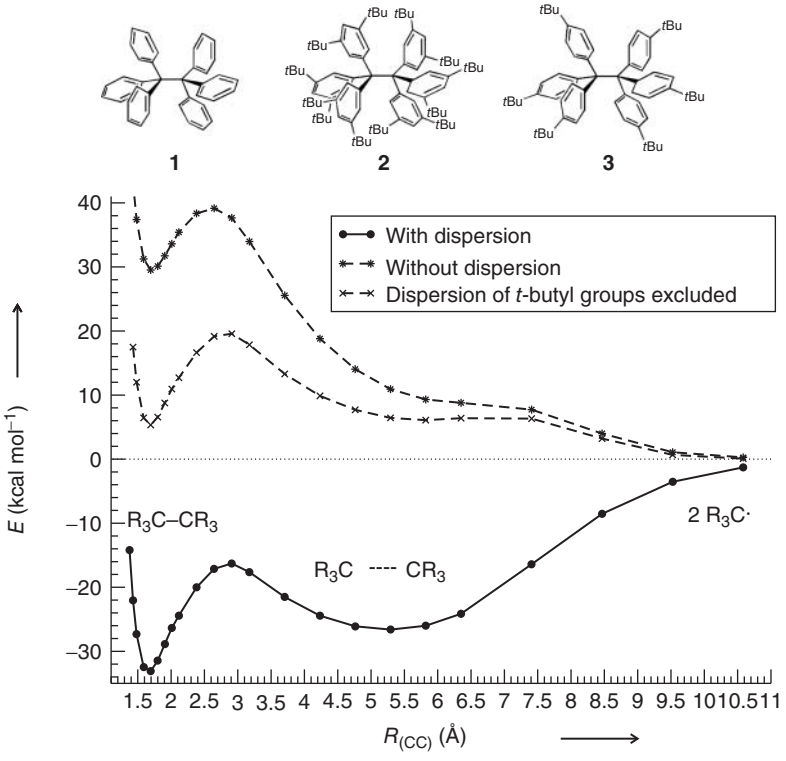

Figure 16.10 Potential energy curves (UTPSS-D3/TZV2P//UPBE-D3/TZVP) for dissociation of the central CC bond in all-meta-*t*-butyl-substituted hexaphenylethane (molecule 2, R = 3,5-di-*t*-butyl-phenyl) with and without dispersion correction. Note the similar depths of the covalent and vdW complex minima in the dispersion-corrected curve and the unbound state (positive interaction energies) without these corrections.

However, why the parent molecule hexaphenylethane cannot be synthesized but the seemingly sterically more overcrowded derivative can be made at least at low temperatures was an open question. The potential energy curves in Figure 16.10 provide the conclusive evidence for the overwhelming role of the dispersion.

The TPSS-D3 curve exhibits two minima at CC distances of 1.67 and 5.28 Å which are connected by a (TS) transition state at R(CC) = 2.87 Å. The minima correspond to the normal covalently bound ethane derivative and a very strong vdW complex of the two radicals. As both minima lie in a comparably deep potential energy well (−33.2 and −26.6 kcal mol^{-1}, respectively), the system can be considered as bond length isomeric. The figure includes data with and without D3-corrections and a curve for which all dispersion arising from the *t*-butyl groups has been set to zero. The uncorrected TPSS curve shows the covalent CC structure and the TS but not the second vdW minimum. Furthermore, the molecular energy is always higher than that of the free radicals, which again emphasizes the importance of dispersion. One of the good features of the DFT-D3 approach is that the dispersion energy can easily be partitioned into different parts or groups of a molecule. The third curve without the *t*-butyl contributions is most remarkable: while its shape is similar to the plain TPSS curve, there is practically no vdW minimum and the interaction energies are positive. Thus, we conclude that the main dispersion stabilization of the experimentally observed compound results from the *t*-butyl groups. The overall repulsive phenyl–phenyl interactions in the parent molecule are overcompensated by addition of ''steric crowding'' in the form of all-meta *t*-butyl groups that do not lead to overcrowding but serve as ''dispersion energy donors.'' The stability of **2** and the instability of **1** as well as **3** can be fully explained on thermodynamic grounds, and all computations agree qualitatively as well as quantitatively with experiment. The dispersion of the *t*-butyl groups stabilizes **2** compared to its radical fragments by as much as 40 kcal mol^{-1}.

16.4.3
Overcoming Coulomb Repulsion in a Transition Metal Complex

Proper tuning of the energetic contribution of dispersion may stabilize molecular aggregates, which would be otherwise highly unstable by virtue of other overwhelming repulsive terms as shown earlier. Literature contains a number of such noncovalently bonded molecular aggregates containing metal (ions), of which the binding mode has never been thoroughly settled. Among those are the emblematic cationic complexes of tetrakis(isonitrile)rhodium(I). The propensity of these complexes to spontaneously produce oligomers has been an open case for years. This very fundamental question as to why two positively charged molecules can form a complex without any significant covalent bonding (which is not possible in the d^8–d^8 configuration of the metal cores) has recently been answered. This example is directly connected to the ES/dispersion discussion (see Figure 16.1) in Section 16.1.

For the dimer $[(PhNC)_4Rh]_2^{2+}$ (see inset in Figure 16.11), one of the archetypes of such oligomers, DFT-D3 and wave-function-based SCS-MP2 [55] quantum

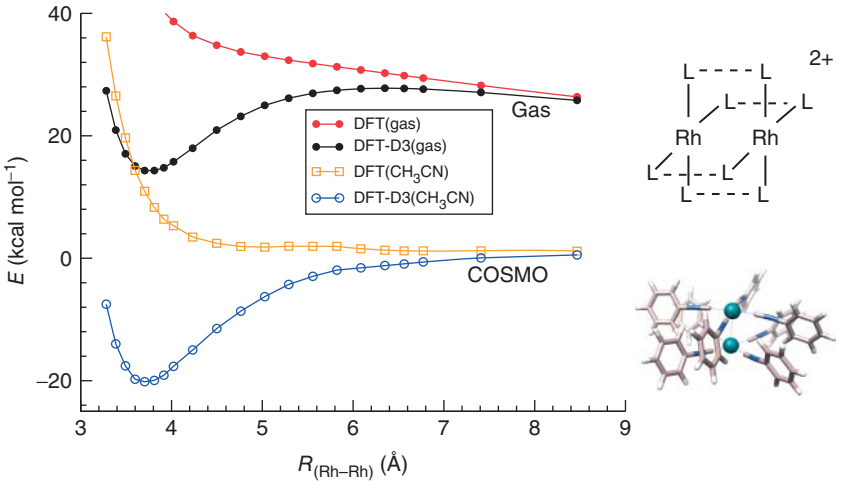

Figure 16.11 Potential energy curves for dissociation of $[(PhNC)_4Rh]_2^{2+}$ along a Rh–Rh bond stretching coordinate at TPSS/def2-TZVP levels. The COSMO continuum solvation model corresponding to the experimentally investigated acetonitrile solution has been applied.

chemical calculations have been performed [14]. These investigations indicate that when the eight isonitrile ligands arrange spatially in an optimal π-stacked manner, the energy due to dispersion not only overcomes coulombic repulsion but also the entropy penalty of complex formation. This central role of long-range electron correlation explains such seeming cation–cation "attractive" interactions. These findings also relativize the role of closed-shell metal–metal "d^8–d^8" interactions, which are present on a relatively small scale compared to the effects of the ligands (only about 10–15% of the total dispersion contribution to the binding energy).

Without dispersion correction, the potentials in the gas phase and with the COSMO continuum solvation correction [79] for acetonitrile are both entirely repulsive (red and orange curves). Because COSMO screens the Coulomb interaction effectively, the DFT+COSMO curve rapidly approaches the asymptote, while in the gas phase it includes the very long-ranged (very slowly decaying) $1/R$ part. But only if COSMO and D3 are added to the bare DFT energies physically plausible potentials result, which correspond to an energetically stable aggregate (which persists even when entropic corrections are added [14]). In the equilibrium region, the dispersion contribution to the binding energy is 20–30 kcal mol^{-1} (>100% of D_e).

16.5 Conclusion

Although the London dispersion interaction has a fundamentally quantum chemical, complex many-particle origin, it is probably the bonding type (or its contribution to bonding) that is easiest to understand. It can be represented accurately by rather

simple models based on ''atoms-in-molecules'' ideas. However, any brute-force wave-function-based *ab initio* quantum chemical treatment of dispersion bonding is ambitious and computationally demanding (because dispersion essentially is a long-range electron correlation effect), but fortunately not necessary in many cases. The reasons for this seeming contradiction are that (a) the dispersion interaction (the quantum effects) operate on a relatively long-range scale where classical (atomic or other local) approximations perform well (and exchange is negligible), (b) it is basically (to within a few percent error) a pair-wise additive property, and (c) the directionality of dispersion bonding is more or less represented by the classical (geometrical) shape of the interacting fragments. Dispersion is a chemically local phenomenon that can be described fairly well by local models of polarizability (excitation energy). However, this mainly holds for insulator-type systems that dominate main group inorganic and organic, as well as biochemistry. For extended metallic systems, the situation is different as these inherently have a NL electronic structure and a clear distinction between short- and long-range correlation is obscured.

Even when dispersion is not sufficient to form a chemical bond, it is clear that larger molecules are significantly more influenced by the intramolecular dispersion energy than smaller ones. Because dispersion is always attractive (energy lowering), this means that larger molecules are thermodynamically stabilized by dispersion compared to small systems. From this it can be concluded that large (preferably electron-rich and polarizable) chemical groups can be used to energetically stabilize weak bonds or reactive parts in a molecule (''dispersion energy donor'' concept). This new thinking about the very old London dispersion theory might be useful as a novel design principle for functional chemical systems.

16.6 Computational Details

The quantum chemical calculations were done with TURBOMOLE (DFT-D3 and CCSD(T)/MP2) [82] and ORCA (DFT-NL) [83, 84]. For the DFT calculations carried out with ORCA and TURBOMOLE, we employed fine integration grids (m4/m5 in TURBOMOLE or grid5 in ORCA) and tight SCF convergence criteria. Where applicable, the resolution of the identity (RI) integral approximation [85, 86] was used. If not stated otherwise, structures were fully optimized at the TPSS-D3(BJ)/def2-TZVP level [38, 40, 42, 69]. For 4d and 5d transition metals the large core (Cologne–Stuttgart) ECP [87, 88] are used.

References

1. IUPAC Gold Book, IUPAC Compendium of Chemical Terminology – the Gold Book, *http://goldbook.iupac.org/V06597.html* (accessed 23 January 2014).
2. London, F. (1930) *Z. Phys.*, **63**, 245–279.
3. Stone, A.J. (1997) *The Theory of Intermolecular Forces*, Oxford University Press, Oxford.

4. Kaplan, I.G. (2006) *Intermolecular Interactions*, John Wiley & Sons, Ltd, Chichester.
5. Hobza, P. (2011) *WIREs Comput. Mol. Sci.*, **1**, 3–17.
6. Lehn, J.-M. (1995) *Supramolecular Chemistry: Concepts and Perspectives*, Wiley-VCH Verlag GmbH, Weinheim.
7. Meyer, E.A., Castellano, R.K., and Diederich, F. (2003) *Angew. Chem. Int. Ed.*, **42**, 1210–1250.
8. Kannan, N., and Vishveshwara, S. (2000) *Protein Eng.*, **13**, 753–761.
9. Desiraju, G.R., Vittal, J., and Ramanan, A. (2011) *Crystal Engineering: A Textbook*, World Scientific Publishing, Singapore.
10. Grimme, S., Huenerbein, R., and Ehrlich, S. (2011) *ChemPhysChem*, **12**, 1258–1261.
11. Dalrymple, D.L., Reinheimer, J.D., Barnes, D., and Baker, R. (1964) *J. Org. Chem.*, **29**, 2647–2652.
12. Pyykkö, P. (1997) *Chem. Rev.*, **97**, 597–636.
13. Grimme, S., and Schreiner, P.R. (2011) *Angew. Chem. Int. Ed.*, **50**, 12639–12642.
14. Grimme, S., and Djukic, J.P. (2011) *Inorg. Chem.*, **50**, 2619–2628.
15. Slavicek, P., Kalus, R., Paska, P., Odvarkova, I., Hobza, P., and Malijevsky, A. (2003) *J. Chem. Phys.*, **119**, 2102–2118.
16. Dobson, J.F., White, A., and Rubio, A. (2006) *Phys. Rev. Lett.*, **96**, 073201.
17. Ruiz, V.G., Liu, W., Zojer, E., Scheffler, M., and Tkatchenko, A. (2012) *Phys. Rev. Lett.*, **108**, 146103.
18. Carrasco, J., Klimes, J., and Michaelides, A. (2013) *J. Chem. Phys.*, **138**, 024708.
19. Kohn, W., and Sham, L.J. (1965) *Phys. Rev.*, **140**, A1133–A1138.
20. Parr, R.G., and Yang, W. (1989) *Density-Functional Theory of Atoms and Molecules*, Oxford University Press, Oxford.
21. Koch, W., and Holthausen, M.C. (2001) *A Chemist's Guide to Density Functional Theory*, Wiley-VCH Verlag GmbH, New York.
22. Cohen, A.J., Mori-Sanchez, P., and Yang, W. (2012) *Chem. Rev.*, **112**, 289–320.
23. Kutzelnigg, W. (1978) *Einführung in die Theoretische Chemie: Band 2, Die chemische Bindung*, Verlag Chemie, Weinheim.
24. Marinescuc, M. (1997) *Phys. Rev. A*, **56**, 4764.
25. Vydrov, O.A., and Van Voorhis, T. (2010) *J. Chem. Phys.*, **133**, 244103.
26. Hujo, W., and Grimme, S. (2011) *J. Chem. Theor. Comput.*, **7**, 3866–3871.
27. Kolos, W., and Wolniewicz, L. (1965) *J. Chem. Phys.*, **43**, 2429.
28. von Hopffgarten, M., and Frenking, G. (2012) *WIREs Comput. Mol. Sci.*, **2**, 43–62.
29. Morokuma, K. (1971) *J. Chem. Phys.*, **55**, 1236–1244.
30. Kitaura, K., and Morokuma, K. (1976) *Int. J. Quantum Chem.*, **10**, 325–340.
31. Bickelhaupt, F.M., and Baerends, E.J. (2000) in *Reviews in Computational Chemistry*, Vol. 15 (eds K.B. Lipkowitz, and D.B. Boyd), Wiley-VCH Verlag GmbH, New York, pp. 1–86.
32. Swart, M., Fonseca Guerra, C., and Bickelhaupt, F.M. (2004) *J. Am. Chem. Soc.*, **126**, 16718–16719.
33. Parac, M., Etinski, M., Peric, M., and Grimme, S. (2005) *J. Chem. Theory Comput.*, **1**, 1110–1118.
34. Grimme, S., Antony, J., Schwabe, T., and Mück-Lichtenfeld, C. (2007) *Org. Biomol. Chem.*, **5**, 741–758.
35. Stephan, D.W., and Erker, G. (2010) *Angew. Chem. Int. Ed.*, **49**, 46–76.
36. Grimme, S., Kruse, H., Goerigk, L., and Erker, G. (2010) *Angew. Chem. Int. Ed.*, **49**, 1402–1405.
37. Gilbert, T.M. (2013) *Top. Curr. Chem.*, doi: 10.1007/1282012378.
38. Tao, J., Perdew, J.P., Staroverov, V.N., and Scuseria, G.E. (2003) *Phys. Rev. Lett.*, **91**, 146401.
39. Schäfer, A., Huber, C., and Ahlrichs, R. (1994) *J. Chem. Phys.*, **100**, 5829–5835.
40. Weigend, F., and Ahlrichs, R. (2005) *Phys. Chem. Chem. Phys.*, **7**, 3297–3305.
41. Goerigk, L., and Grimme, S. (2011) *Phys. Chem. Chem. Phys.*, **13**, 6670–6688.
42. Grimme, S., Antony, J., Ehrlich, S., and Krieg, H. (2010) *J. Chem. Phys.*, **132**, 154104.
43. van Gisbergen, S.J.A., Snijders, J.G., and Baerends, E.J. (1995) *J. Chem. Phys.*, **103**, 9347–9354.

44. Osinga, V.P., van Gisbergen, S.J.A., Snijders, J.G., and Baerends, E.J. (1997) *J. Chem. Phys.*, **106**, 5091–5101.

45. Johnson, E.R. (2011) *J. Chem. Phys.*, **135**, 234109.

46. Sulzer, D., Norman, P., and Saue, T. (2012) *Mol. Phys.*, **110**, 2535–2541.

47. Ehrlich, S., Moellmann, J., and Grimme, S. (2012) *Acc. Chem. Res.*, **45**, doi: 10.1021/ar3000844.

48. Hohenstein, E.G., and Sherrill, C.D. (2012) *WIREs Comput. Mol. Sci.*, **2**, 304–326.

49. Kruse, H., and Grimme, S. (2012) *J. Chem. Phys.*, **136**, 154101.

50. Kruse, H., Goerigk, L., and Grimme, S. (2012) *J. Org. Chem.*, **77**, 10824–10834.

51. Helgaker, T., Jørgensen, P., and Olsen, J. (2000) *Molecular Electronic-Structure Theory*, John Wiley & Sons, Inc., New York.

52. Grimme, S., Mück-Lichtenfeld, C., and Antony, J. (2008) *Phys. Chem. Chem. Phys.*, **10**, 3327–3334.

53. Moeller, C., and Plesset, M.S. (1934) *Phys. Rev.*, **46**, 618–622.

54. Cremer, D. (2011) *WIREs Comput. Mol. Sci.*, **1**, 509–530.

55. Grimme, S., Goerigk, L., and Fink, R.F. (2012) *WIREs Comput. Mol. Sci.*, **2**, 868–885.

56. Mulliken, R.S. (1955) *J. Chem. Phys.*, **23**, 1833–1840.

57. Schwabe, T., Grimme, S., and Djukic, J.P. (2009) *J. Am. Chem. Soc.*, **131**, 14156–14157.

58. Ryde, U., Mata, R.A., and Grimme, S. (2011) *Dalton Trans.*, **40**, 11176–11183.

59. Grimme, S. (2011) *WIREs Comput. Mol. Sci.*, **1**, 211–228.

60. Klimes, J., and Michaelides, A. (2012) *J. Chem. Phys.*, **137**, 120901.

61. Becke, A.D., and Johnson, E.R. (2005) *J. Chem. Phys.*, **123**, 154101.

62. Tkatchenko, A., and Scheffler, M. (2009,) *Phys. Rev. Lett.*, **102**, 073005.

63. Dion, M., Rydberg, H., Schröder, E., Langreth, D.C., and Lundqvist, B.I. (2004) *Phys. Rev. Lett.*, **92**, 246401.

64. Lin, Y., Li, G., Mao, S., and Chai, J. (2013) *J. Chem. Theory Comput.*, **9**, 263–272.

65. Heßelmann, A. (2013) *J. Chem. Theory Comput.*, **9**, 273–283.

66. Casimir, H.B.G., and Polder, D. (1948) *Phys. Rev.*, **4**, 360–372.

67. Krishtal, A., Geldorf, D., Vanommeslaeghe, K., Alsenoy, C.V., and Geerlings, P. (2012) *J. Chem. Theory Comput.*, **8**, 125–134.

68. Ehrlich, S., Moellmann, J., Reckien, W., Bredow, T., and Grimme, S. (2011) *ChemPhysChem*, **12**, 3414–3420.

69. Grimme, S., Ehrlich, S., and Goerigk, L. (2011) *J. Comput. Chem.*, **32**, 1456–1465.

70. Rezáč, J., Riley, K.E., and Hobza, P. (2011) *J. Chem. Theory Comput.*, **7**, 2427.

71. Koide, A. (1976) *J. Phys. B*, **9**, 3173.

72. Burns, L.A., Vazquez-Mayagoitia, A., Sumpter, B.G., and Sherrill, C.D. (2011) *J. Chem. Phys.*, **134**, 084107.

73. Goerigk, L., Kruse, H., and Grimme, S. (2011) *ChemPhysChem*, **12**, 3421–3433.

74. Ott, I., and Gust, R. (2007) *Anti-Cancer Agents Med. Chem.*, **7**, 95–110.

75. Szalewicz, K. (2012) *WIREs Comput. Mol. Sci.*, **2**, 254–272.

76. Sherrill, C.D. (2009) in *Reviews in Computational Chemistry*, Vol. 26 (eds K.B. Lipkowitz, and D.B. Boyd), Wiley-VCH Verlag GmbH, New York, pp. 1–39.

77. Hohenstein, E.G., and Sherrill, C.D. (2010) *J. Chem. Phys.*, **133**, 104107.

78. Lao, K.U., and Herbert, J.M. (2013) *J. Phys. Chem. Lett.*, **3**, 3241–3248.

79. Klamt, A., and Schüürmann, G. (1993) *J. Chem. Soc., Perkin Trans. 2*, 799–805.

80. Klamt, A. (1995) *J. Phys. Chem.*, **99**, 2224–2235.

81. Klamt, A. (2011) *WIREs Comput. Mol. Sci.*, **1**, 699–709.

82. TURBOMOLE, Ahlrichs, R. *et al.* (2009) Universität Karlsruhe 2009, *http://www.turbomole.com* (accessed 23 January 2014).

83. Neese, F. (2011) *ORCA - An Ab Initio, Density Functional and Semiempirical Program Package, Version 2.9 (Rev 0)*, Max Planck Institute for Chemical Energy Conversion, Germany.

84. Neese, F. (2012) *WIREs Comput. Mol. Sci.*, **2**, 73–78.

85. Vahtras, O., Almlöf, J., and Feyereisen, M.W. (1993) *Chem. Phys. Lett.*, **213**, 514–518.

86. Weigend, F., and Häser, M. (1997) *Theor. Chem. Acc.*, **97**, 331–340.

87. *http://www.theochem.uni-stuttgart.de/pseudopotentials/index.en.html*, *http://www.tc.uni-koeln.de/PP/index.en.html* (accessed 23 January 2014)

88. Dolg, M., and Cao, X. (2012) *Chem. Rev.*, **112**, 404–480.